January 2015

Reconstructing Neuronal Connectivity From Calcium Imaging Data Using Generalized Transfer Entropy

Jina Li
Yale University, jinali.berkeley@gmail.com

Reconstructing neuronal connectivity from calcium imaging data using generalized transfer entropy

Jina Li

May 1, 2015

Abstract

The reconstruction of neuronal connectivity is a very interesting and important topic in neuroscience as it helps with understanding neuronal circuit and function. With the advancement of calcium fluorescence imaging technique, we can now observe the dynamical activity of hundreds of neurons *in vivo* in one setting, which provides a foundation for inferring connectivity within a community or network. Poor signal-to-noise ratio and low frame rate with respect to neurons' actual firing rate are challenges that come with calcium imaging data. Here we review several methods that can be applied to calcium imaging data, without the direct need for converting the data to spike trains which is the more traditional and popular way of connectivity analysis. We then apply generalized transfer entropy to three different sets of calcium imaging data obtained from mice visual cortex, and infer the directed functional connectivity network, in which a directed edge implies a direct causal influence by source neuron to sink neuron. The transfer entropy causal influence measure is time-dependent but requires no prior statistical assumptions on neuron firing patterns and network topology, hence model-free and applicable in face of aforementioned challenges. The performance of this measure has previously been tested on simulated data, and its performance applied to real data, as is the case in this project, is assessed using randomization. We found using properties of randomized networks compared with properties of our reconstructed network that transfer entropy was able to identify significant non-random features of the imaging data. Therefore, the inferred connectivity can provide information on the functional organization of the neuronal networks.

Acknowledgement

This project has enabled me to go beyond my scope of biological and statistical knowledge and explore a vastly different but highly enlightening field of science. The experience has been extremely rewarding. I would not have been able to garner such a wonderful opportunity without the support of the entire faculty and staff here at Yale School of Public Health.

In particular, I would like to thank my thesis advisor and first reader, Dr. Denise Esserman, who provided me with immense help towards the completion of this thesis. I would like to thank my second reader and principal investigator, Dr. Mike Higley, whose knowledge and empathy towards students created an extremely affable learning environment. Many thanks to my academic advisor Dr. Peter Peduzzi who originally provided me with this opportunity, Dr. Forrest Crawford for his patience and ability to deal with my spontaneous questions regarding this topic, and Dr. Meredith Stowe's and Dr. Robert Makuch's caring and supportive mentorship.

Finally, I would like to thank my family and friends, especially Yiming Hu and Amy Zhang, for their understanding and undying support during these past months.

Table of Contents

List of Figures

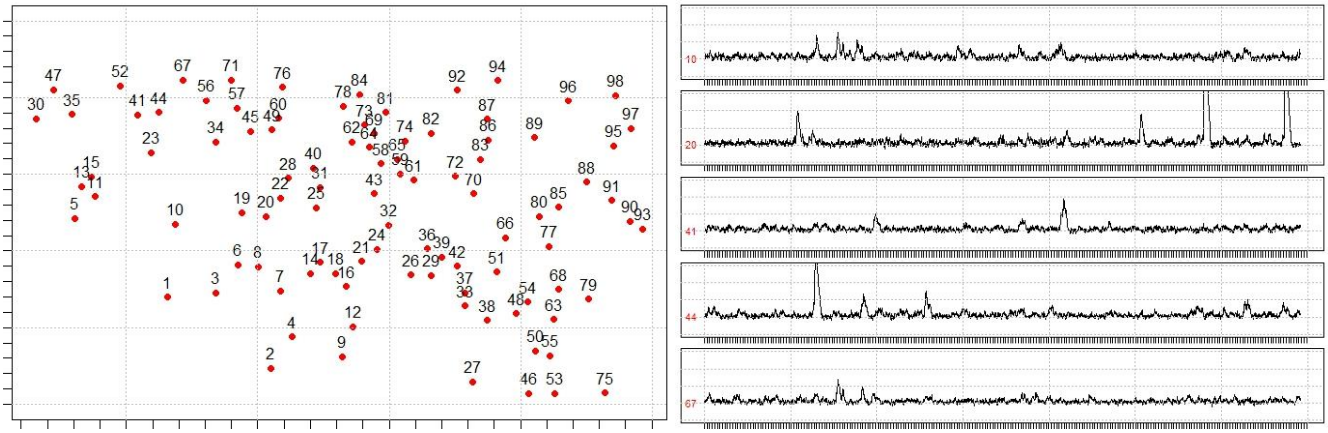

Figure 1. (left) **x-y coordinates** of 98 neurons in the first dataset; (right) **Examples** of neuron calcium fluorescence traces in the form $\Delta F/F$ recorded for over 230+ seconds at 14.8Hz

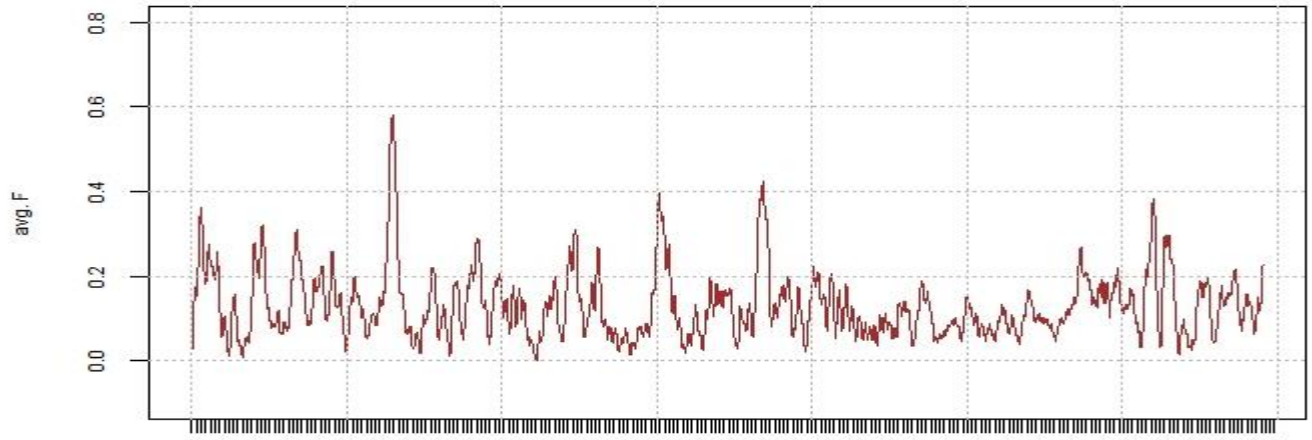

Figure 2. **Average** $\Delta F/F$ traces of whole population of neurons (N=98) over 230+ seconds

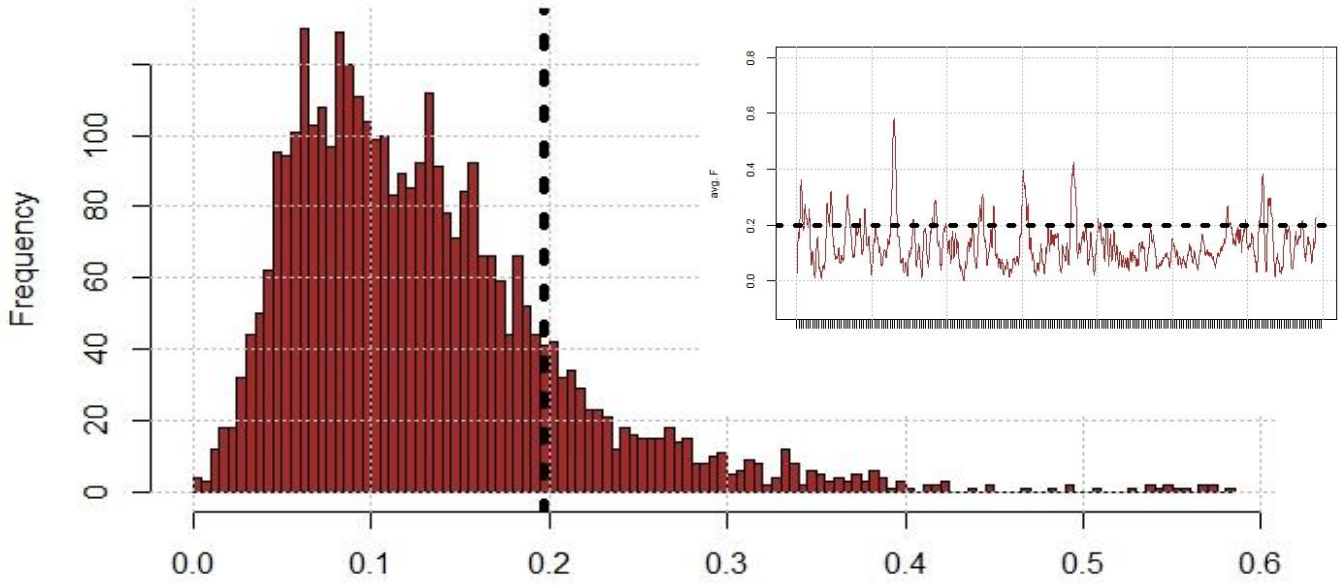

Figure 3. (main) **Distribution of population-averaged** $\Delta F/F$ **amplitudes**; choose $\tilde{g} = 0.1974$; (top-right) **Figure 2 re-plotted** to show average fluorescence values above and below conditioning level $\tilde{g}$. We use time points in our dataset for which the overall average at that time point is strictly less than this level

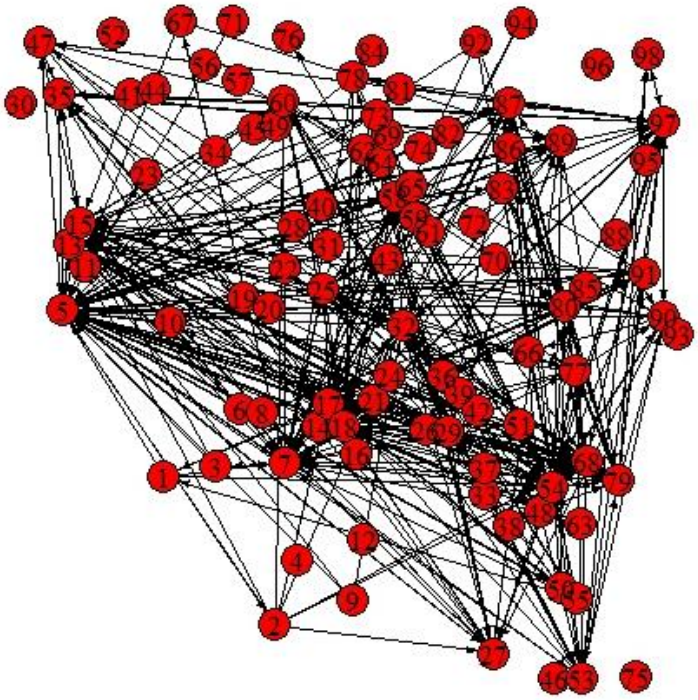

Figure 4. Reconstructed connectivity (k=2) of dataset 1 using pre-processed neuropil-corrected $\Delta F/F$. Reconstruction evaluated for S=1, B=4, k=2, and conditioning level=0.1974. Graph reflects thresholding which retained top 5% of links. Average full cluster coefficient is found to be 0.182 and average in-degree for all nodes (neurons) is approximately 5

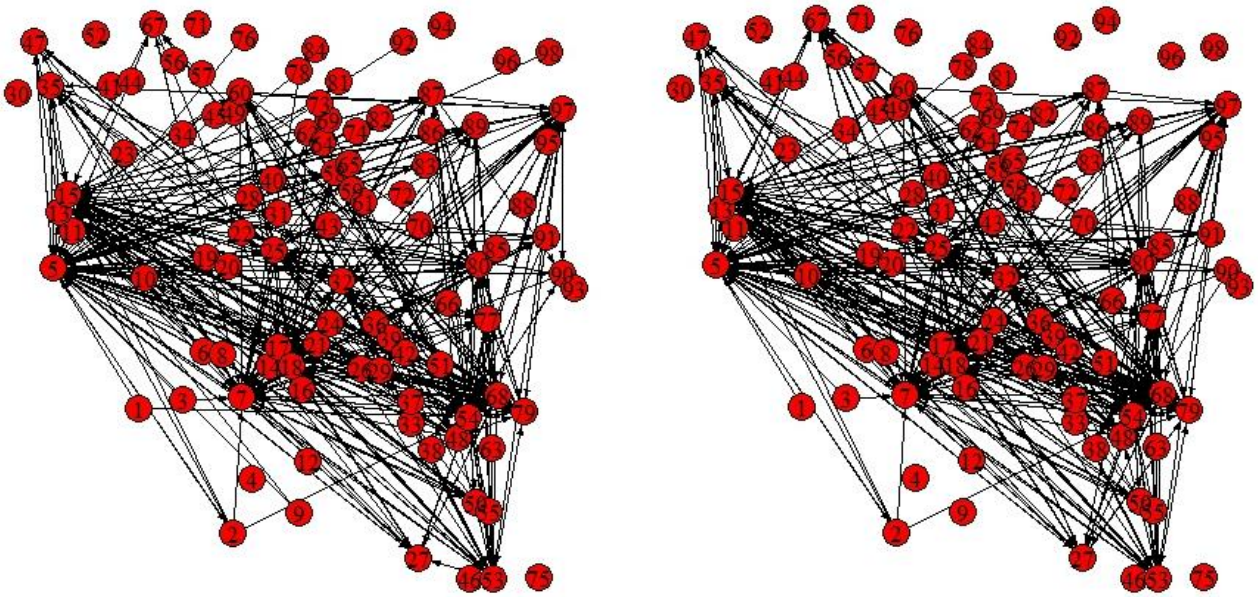

Figure 5. Reconstructed connectivity (k=3, k=4) of dataset 1 using pre-processed neuropil-corrected $\Delta F/F$. Reconstruction evaluated for S=1, B=4, conditioning level=0.1974, and k = 3 (left) or k = 4 (right). Graph reflects thresholding which retained top 5% of links. Average full cluster coefficient is found to be 0.180 for k=3, and 0.146 for k=4. The average in-degree for all nodes is 5 for both k=3 and k=4

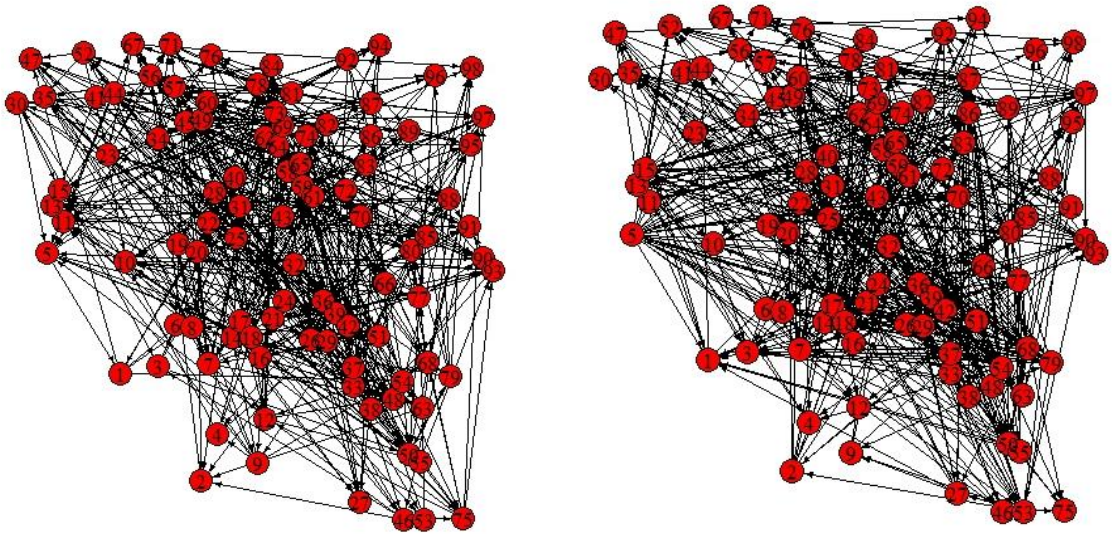

Figure 6. (left) **Reconstructed connectivity from randomization of k=2 adjacency matrix**. Average full cluster coefficient found to be 0.024; (right) **Reconstructed connectivity from partial randomization of k=2 adjacency matrix**, preserving out-degree, exploring randomness of in-degree. Average full cluster coefficient found to be 0.045

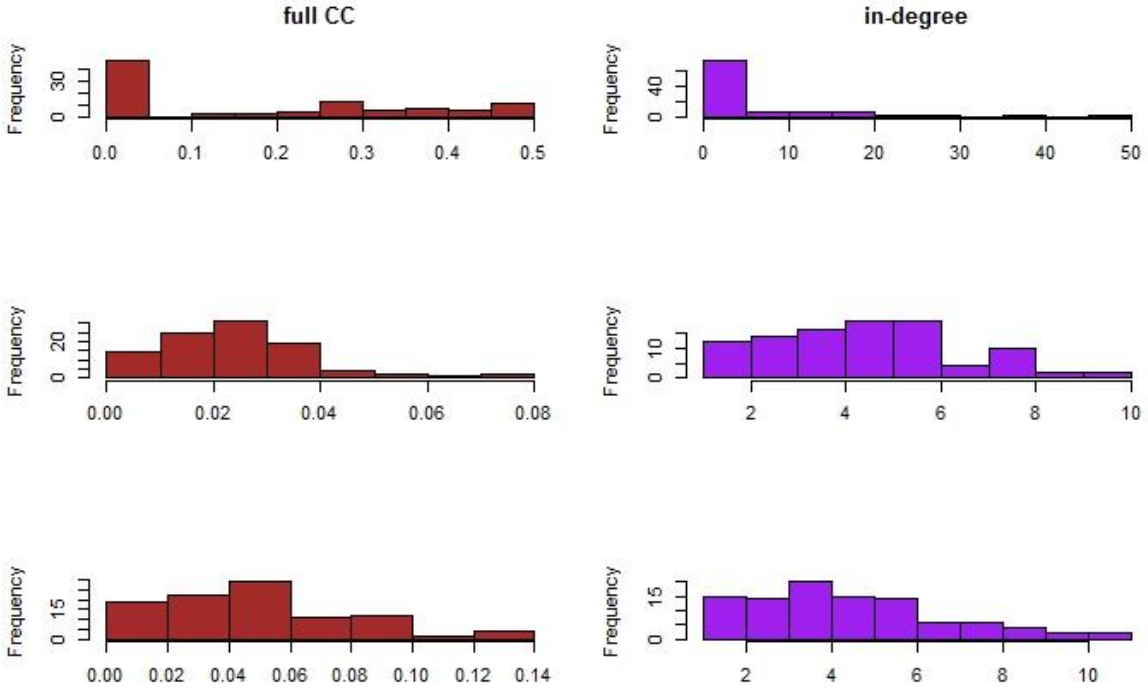

Figure 7a. Properties of network reconstructed from GTE (top row) compared to randomized network (middle row) and partially randomized network (bottom row)

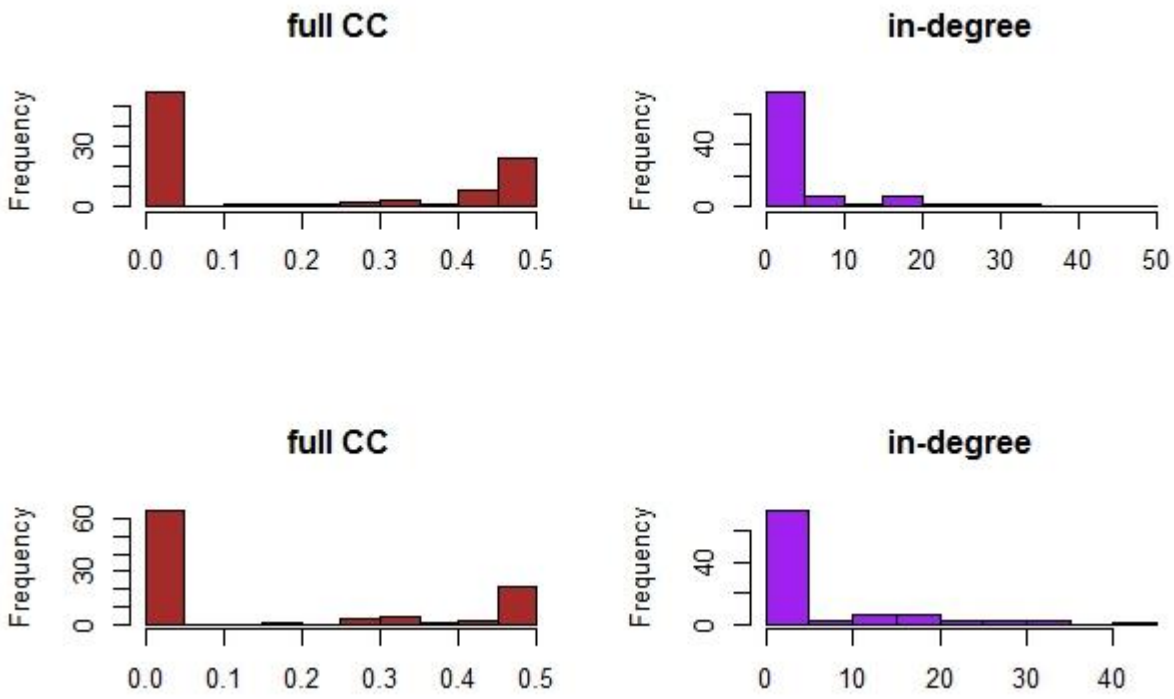

Figure 7b. Properties of network reconstructed from GTE with k=3, number of nodes with no in-degrees found to be 64 (top-row); compared to reconstructed network from GTE with k=4, number of nodes with no in-degree found to be 67 (bottom row)

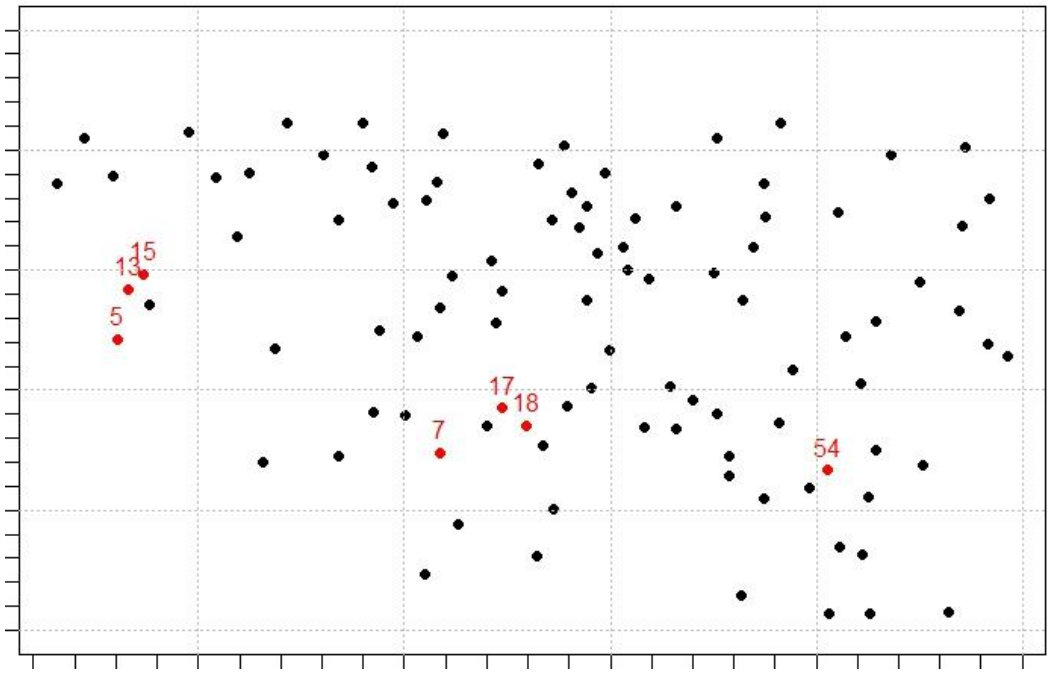

Figure 8. Hubs of causal connectivity: sink nodes defined as having larger than average in-degrees are highlighted in red (with 20 or more in-degrees). Cross-correlation can be used to find the relative strength of synchrony within a local hub (causal link node and each immediate neighbors), and then compared and tested against peak cross-correlations over the entire population

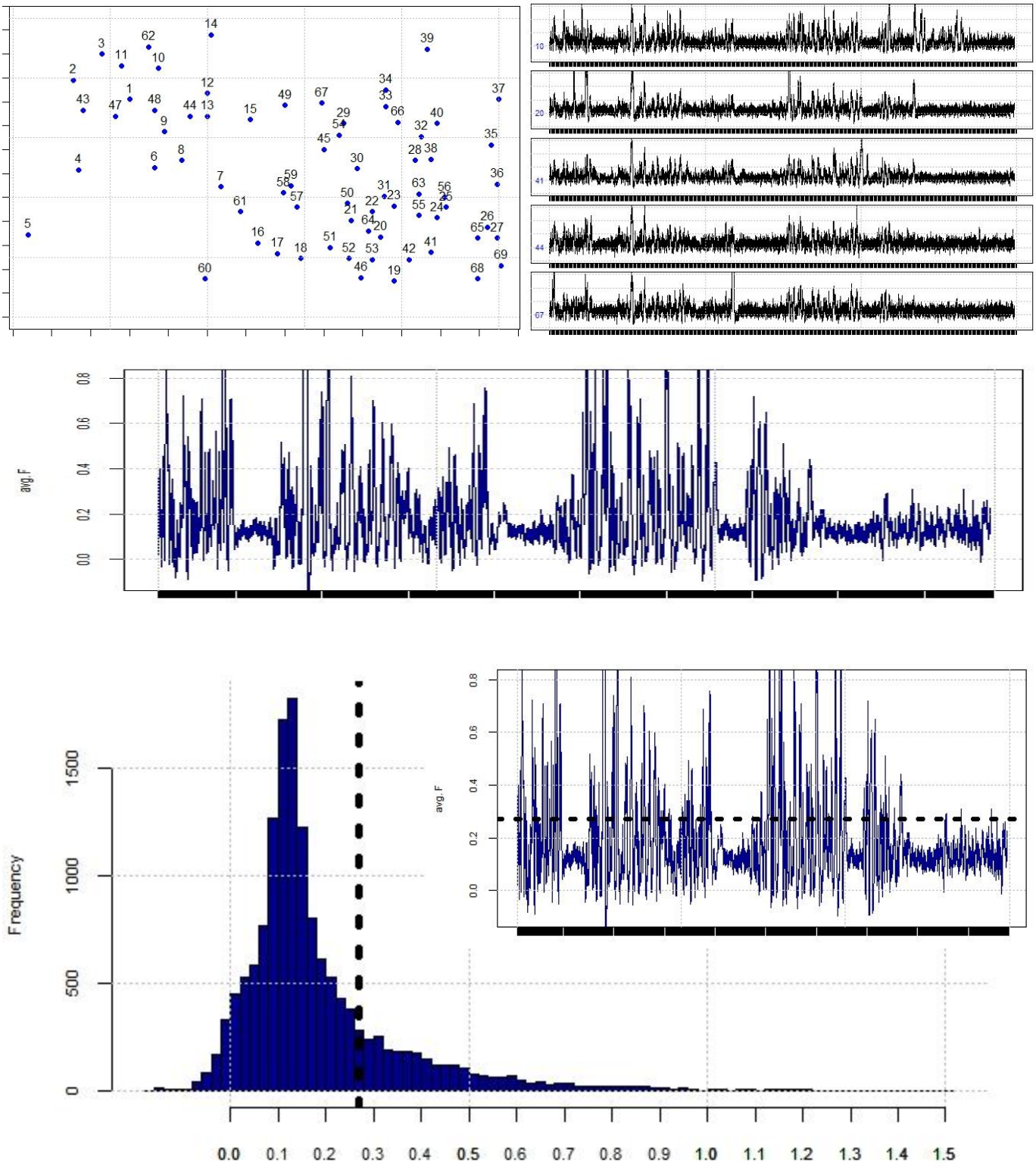

Figure 9. (top-left) **x-y coordinates** of 69 neurons in the second dataset; (top-right) **Examples** of neuron calcium fluorescence traces in the form $\Delta F/F$ (window = 3s, lowest 30%) recorded for over 500+ seconds at 28.38Hz; (middle) **Average $\Delta F/F$ traces of whole population** of neurons (N=69) over 500+ seconds; (bottom main) **Distribution of population-averaged $\Delta F/F$ amplitudes**; choose $\tilde{g} = 0.2703$; (bottom-right) **Average $\Delta F/F$** re-plotted to show average fluorescence values above and below conditioning level $\tilde{g}$. We use time points in our dataset for which the overall average at that time point is strictly less than this level

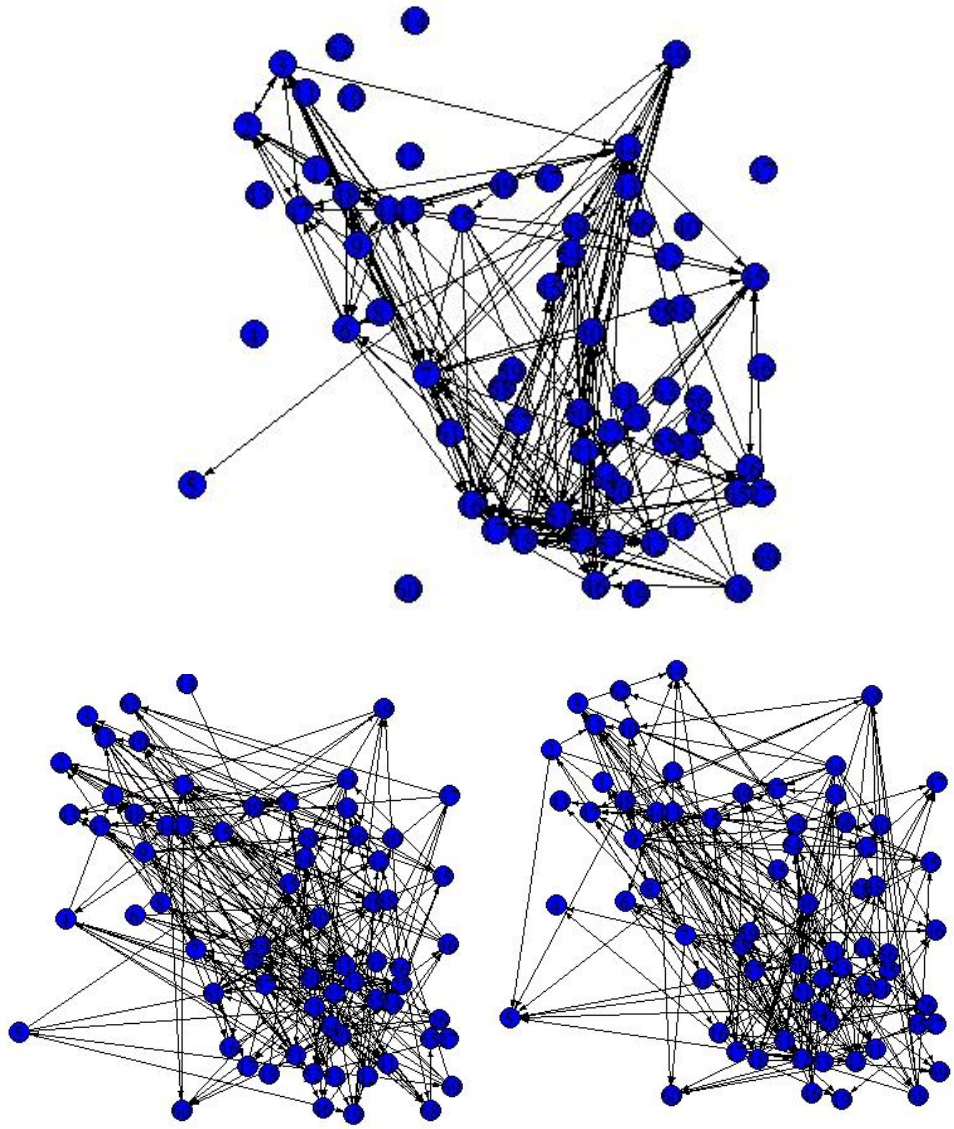

Figure 10. (top) **Reconstructed connectivity** of dataset 2 using pre-processed $\Delta F/F$. Reconstruction evaluated for S=1, B=4, k=2, and conditioning level=0.2703. Graph reflects thresholding which retained top 5% of links. Average full cluster coefficient was found to be 0.107 and average in-degree for all nodes (neurons) is approximately 3.5; (bottom left) **Reconstructed connectivity from randomization of adjacency matrix**. Average full cluster coefficient found to be 0.024; (bottom right) **Reconstructed connectivity from partial randomization of adjacency matrix**, preserving out-degree, exploring randomness of in-degree. Average full cluster coefficient found to be 0.046

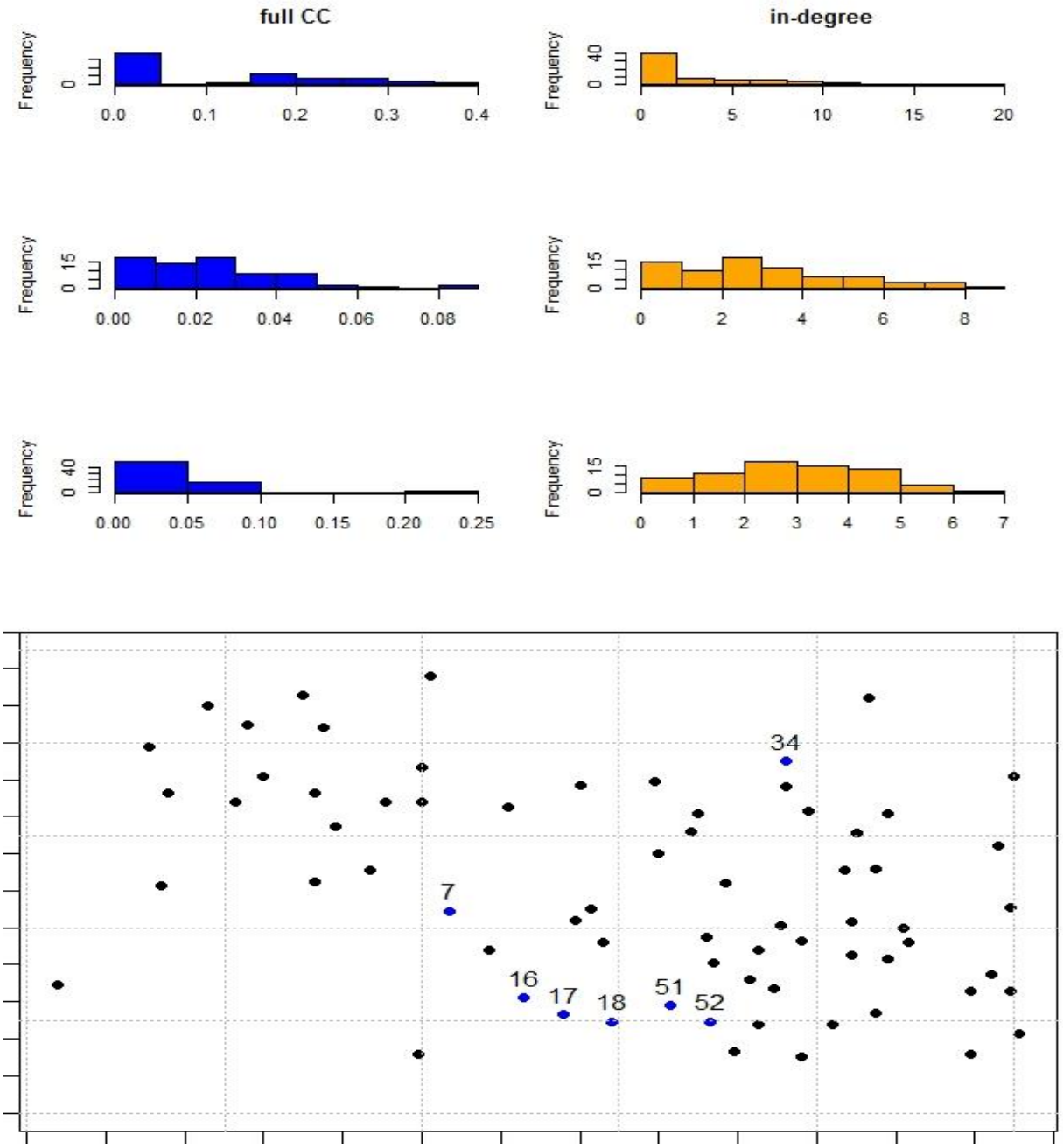

Figure 11. (top) **Properties of network** reconstructed from GTE (top row) compared to randomized network (middle row) and partially randomized network (bottom row); (bottom) **Hubs of causal connectivity:** sink nodes with 10 or more in-degrees are highlighted in blue

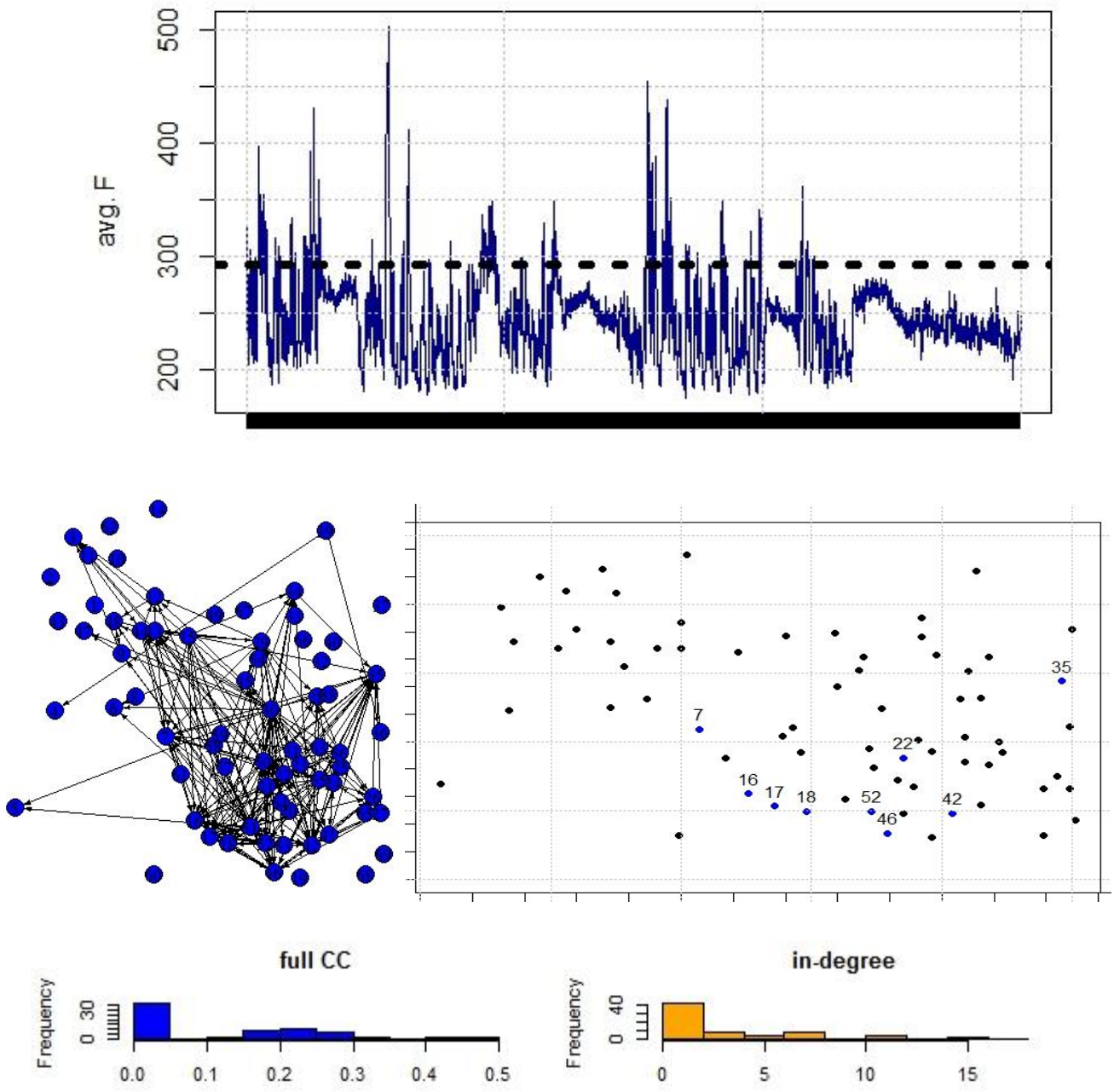

Figure 12. (top**) Conditioning level** chosen based on population-averaged raw data; (middle-left) **reconstructed connectivity** of dataset 2 using raw data (non-processed). Reconstruction evaluated for S=1, B=4, k=2, and conditioning level=292.33. Graph reflects thresholding which retained top 5% of links. Average full cluster coefficient was found to be 0.116 and average in-degree for all nodes (neurons) is approximately 3.5; (middle-right) **Sink nodes with 10 or more in-degrees** are highlighted in blue; (bottom) **Properties of network** distribution of full cluster coefficient and in-degrees

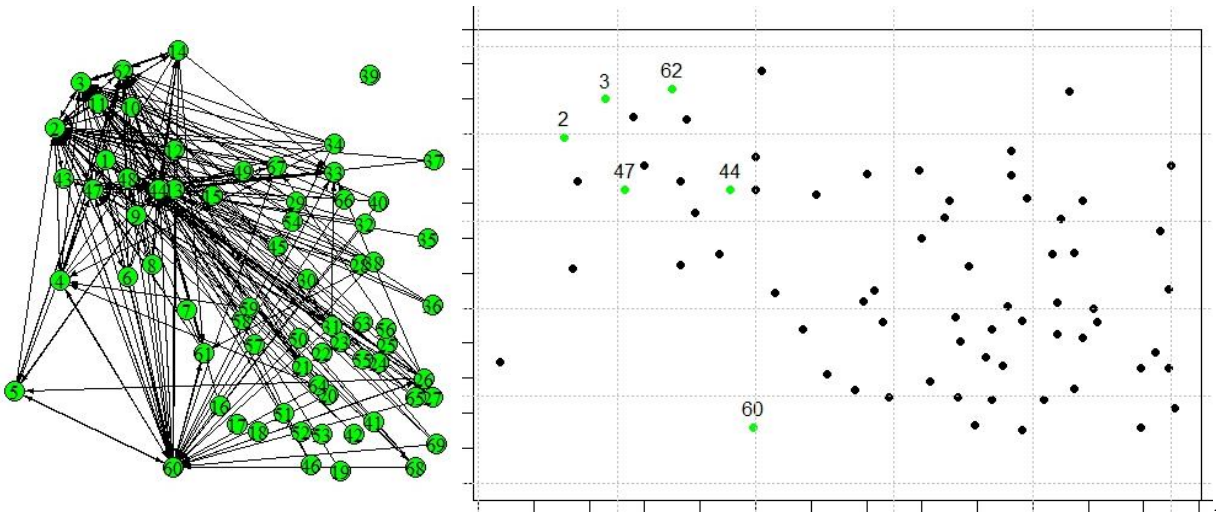

A. 0.275

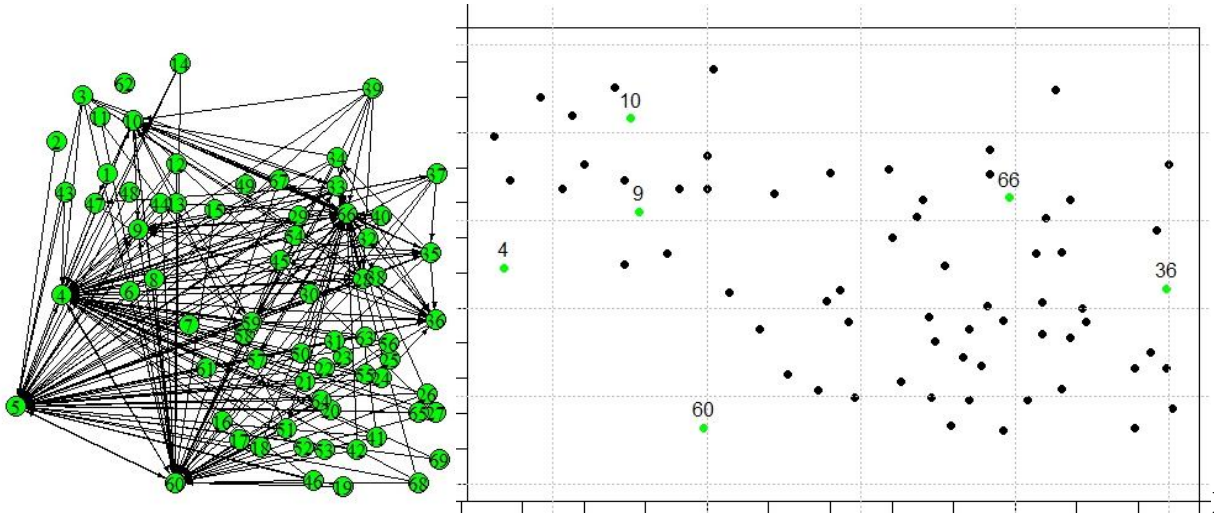

B. 0.329

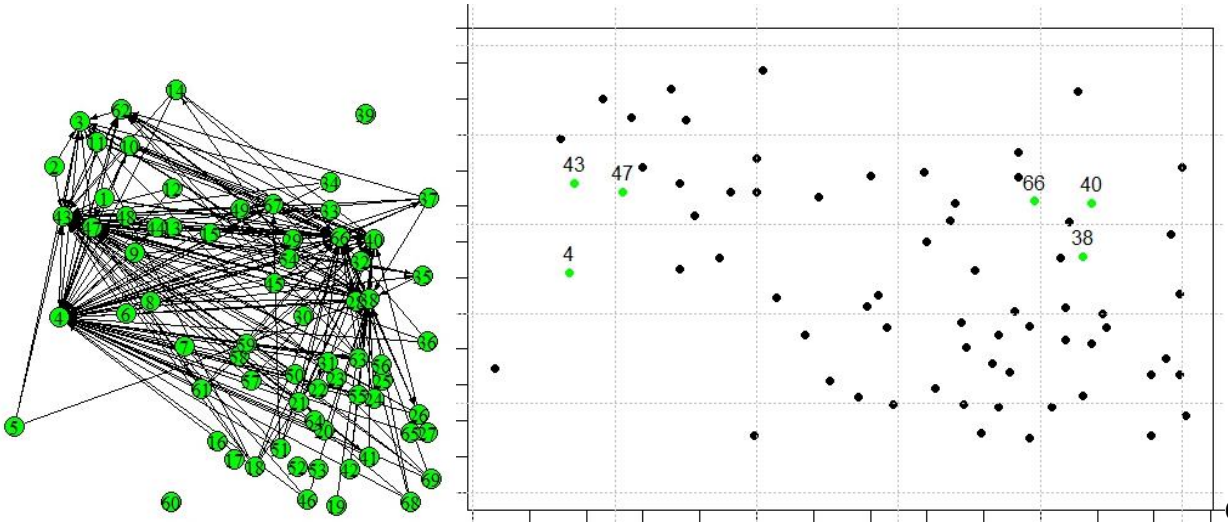

C. 0.311

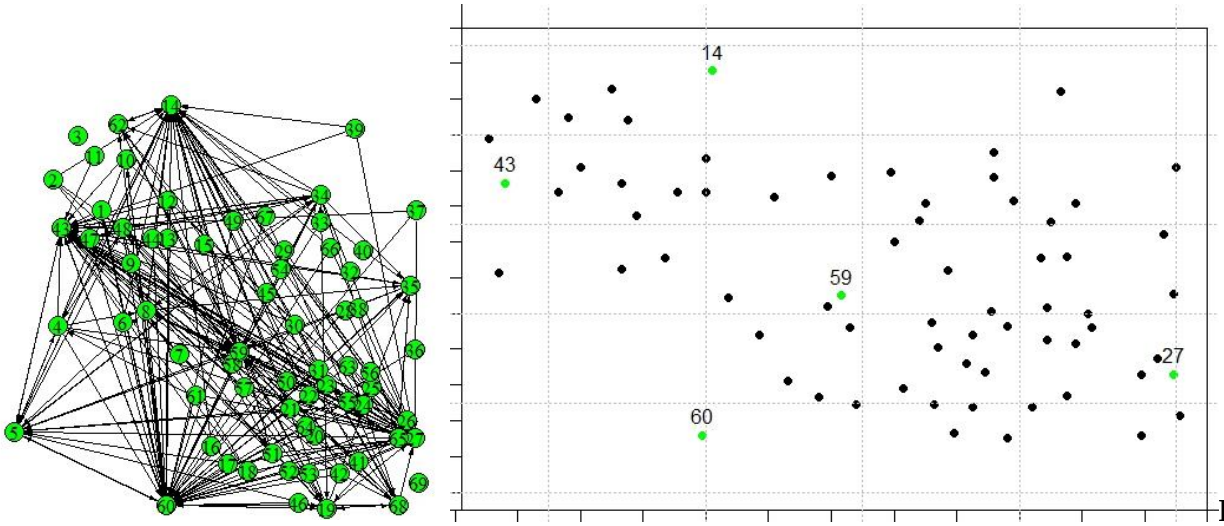

D. 0.245

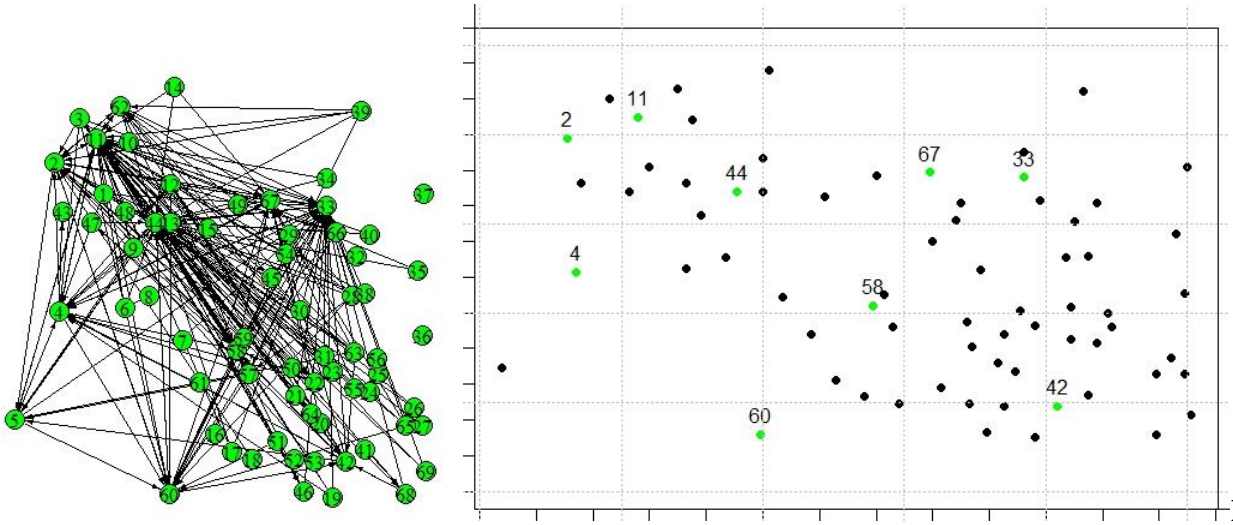

E. 0.242

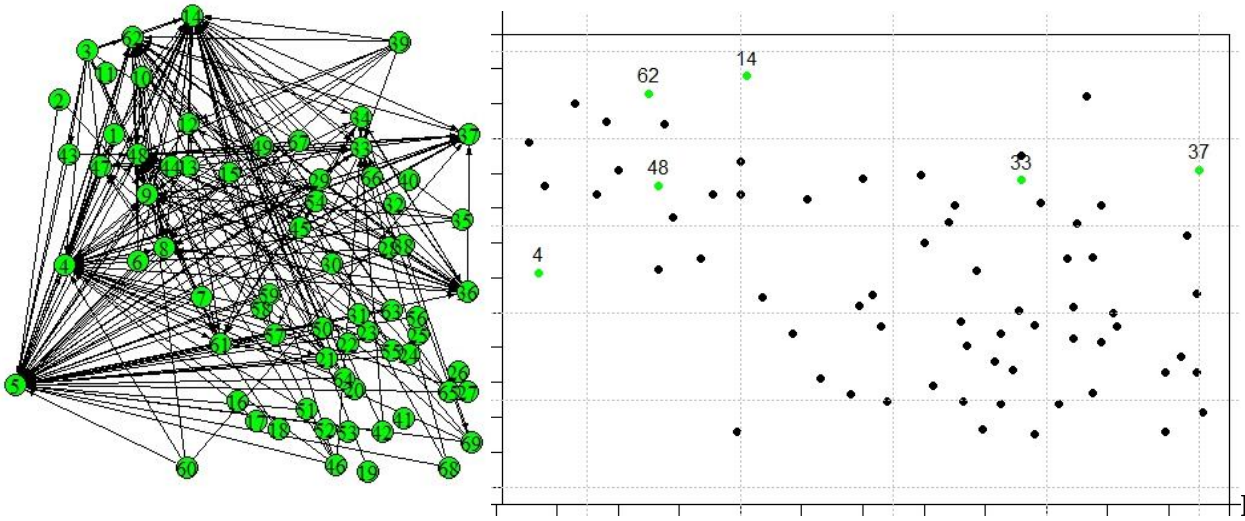

F. 0.207

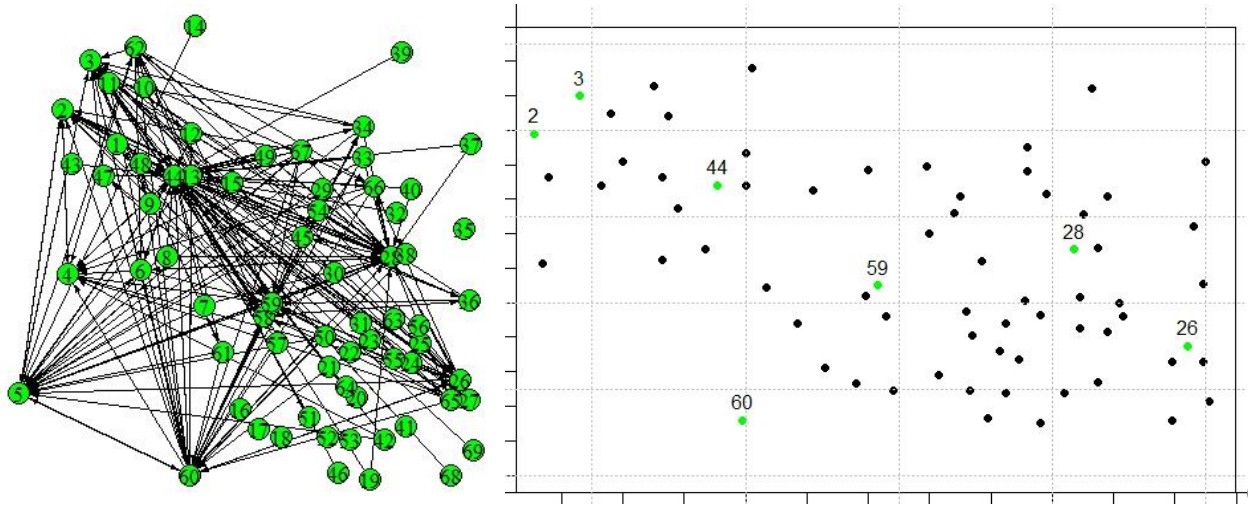

G. 0.228

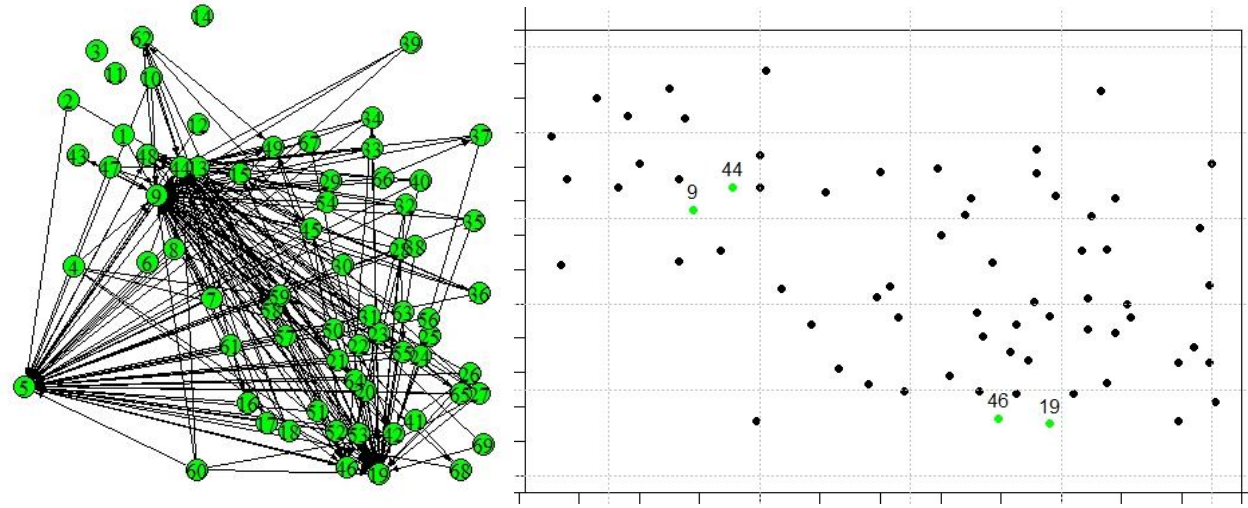

H. 0.308

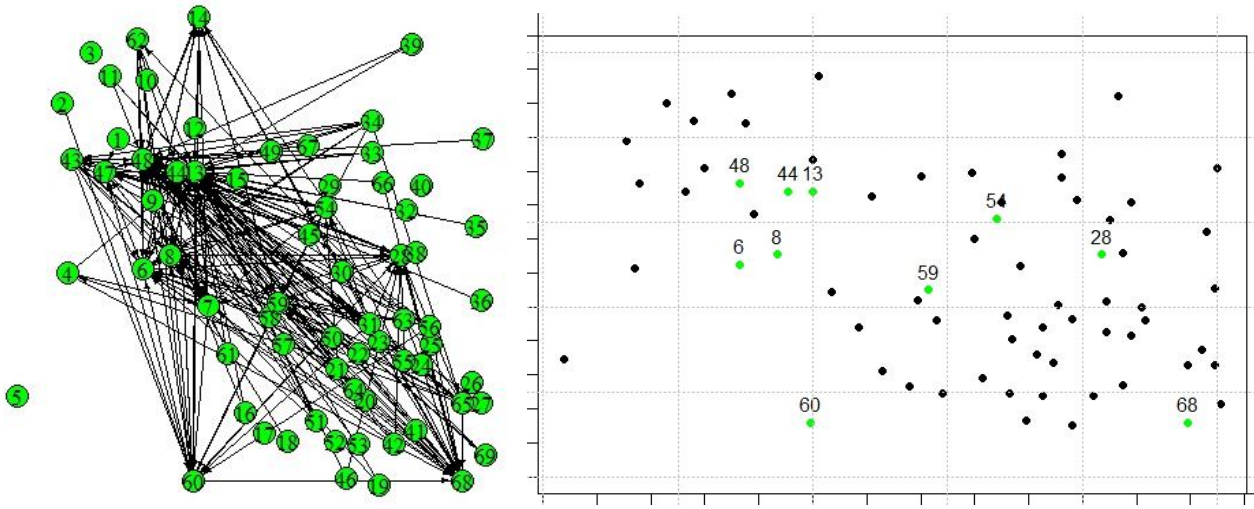

I. 0.208

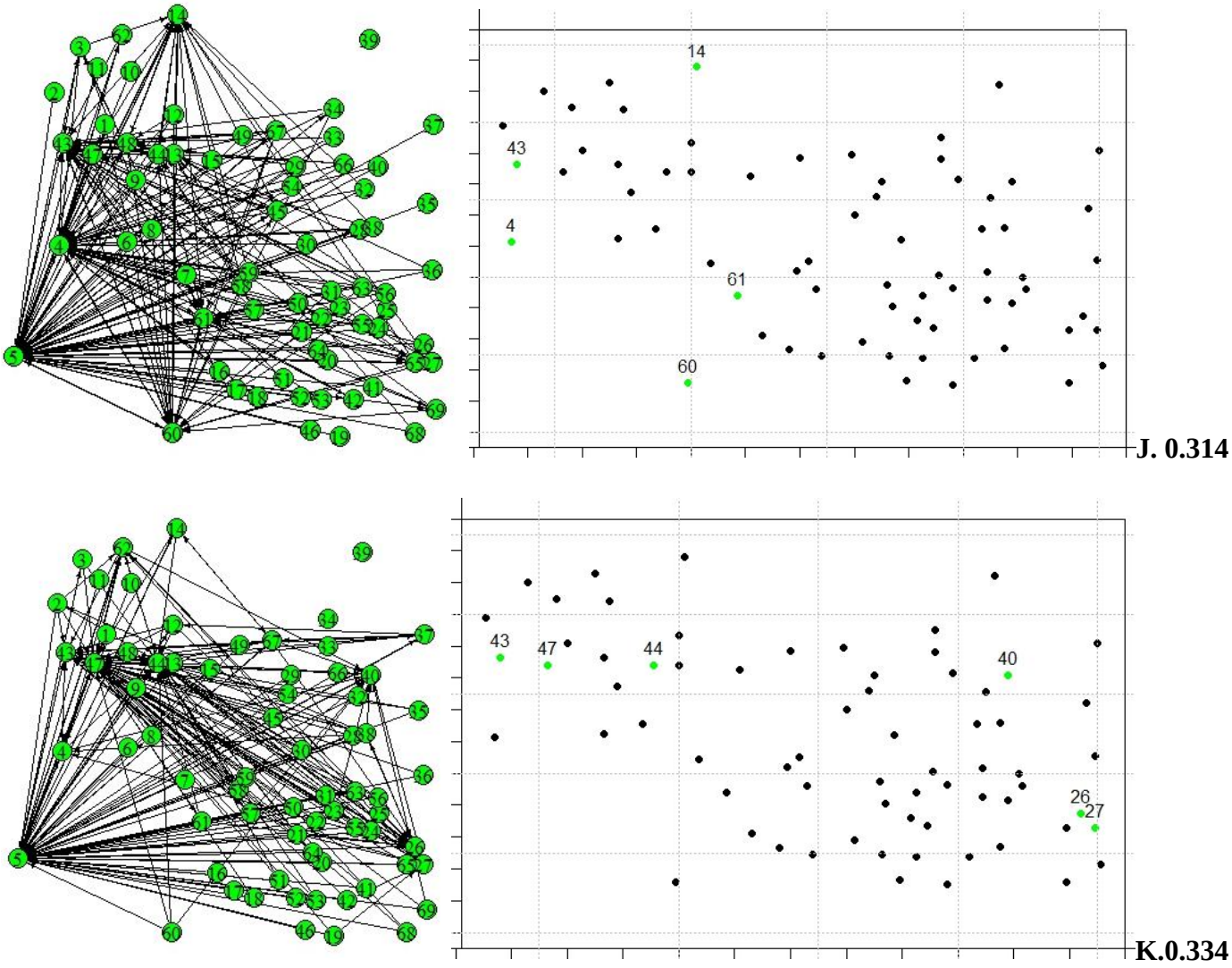

Figure 13. (left column) **Reconstructed connectivity of Stimulus data**, for 11 levels (indicated by letters A-K) of contrasts, using pre-processed $\Delta F/F$. In each reconstruction, 69 neurons over approximately 178 image frames (at 28.38 Hz) were used. Reconstruction evaluated for S=1, B=4, k=2 with no conditioning level (as data is already limited). Graphs reflect thresholding which retained top 5% of links. Average full cluster coefficient for each contrast level is listed beside each row, and the average in-degree is always 3.5; (right column) **Hubs of causal connectivity:** sink nodes with 10 or more in-degrees are highlighted in green for each contrast level

1. Introduction

During the past century neuroscientists have tried to understand the mechanism for memory, cognition, and perception by studying the connectivity between different brain regions. Now, with the help of more promising technology (Stevenson & Kording, 2011), studying populations of neurons at the cellular level has become of great interest (Mishchencko, Vogelstein, & Paninski, 2011). Of many, one important problem concerning populations of neurons is how neurons work together to form a functioning system, be it to encode information or to communicate. A popular way to assess collective behavior is to study population coding (Montijn, Vinck, & Pennartz, 2014) using signal correlation between neurons and trial-to-trial variability in the responses of multiple neurons over repeats of the same stimulus, called noise correlations (i.e. repeat presentations of the same stimulus results in different responses on each trial, and this variability can be correlated across different neurons) (Zylberberg & Shea-Brown, 2014). However, studies on neuronal correlation to date have reported discrepant findings (Cohen & Kohn, 2013). Another way, complimentary to neuronal correlation and factors in a lot more temporal information, is to identify topological features of the network. In other words, to infer circuits or connectivity within the network based on neurons' activity time series. This, in turn, can be essential to understanding the structure of networks and how neurons in them compute and function (Stetter, Battaglia, Soriano, & Geisel, 2012). In this paper we will study the topological features of a population of neurons. Our aim is to reconstruct the connectivity based on the population's dynamical activity to see if the population of neurons have any interaction with each other.

There are many available experimental tools to capture neuron activities, such as the extracellular electrodes (EEG). However, tools like EEG are inadequate for capturing the synaptic activities of many neighboring neurons simultaneously, as the electrodes can only be placed so closely (Mishchencko, Vogelstein, & Paninski, 2011). In neurons, the movement of calcium ions is how bioelectrical currents are generated and propagated, and thus calcium imaging techniques have become of popular use. Scientists can now study neuron activities simultaneously in dozens to hundreds of neighboring neurons, by bulk-loading calcium-sensitive fluorescence indicators into the brain tissue and measuring the changes of fluorescence using imaging technique.

However, this technique also has its disadvantages. This technique can have low temporal resolution, which means that the frame rate of image acquisition is much slower than the firing dynamic of neurons (Stetter, Battaglia, Soriano, & Geisel, 2012). Additionally, the fluorescence reaction to the calcium indicator is not immediate, as well the bright of the neuron decays at an order of magnitude slower than the time of the actual neuronal activity, decreasing signal-to-noise ratio (Rama, 2013). To analyze the collected data effectively, some advanced and/or efficient statistical methods specifically for calcium imaging data have been developed. In the next section we will briefly explain three methods, of which generalized transfer entropy will be used to analyze our sets of real data.

2. Review of Methods

In reconstructing connectivity, there exists deconvolution methods that go to great lengths to extract spike trains (series of discrete action potentials from a neuron taken as a time series) from imaging time series as a pre-processing step (Garofalo, Nieus, Massobrio, & Martinoia, 2009). In this paper we will focus on methods that do not directly go through this step. The following Bayesian approach includes this step in its model rather than in the pre-processing step. There also exists methods that operate directly on time series acquired from imaging, such as cross-correlation and transfer entropy, without the need for deconvolution. Though some sort other basic data pre-processing is necessary.

2.1 Bayesian

The method developed by Mishchencko et al. introduces a Markovian state-space model that relates the fluorescence time sequence as a non-linear function of Calcium activity to its hidden states, the spike train. It then uses a Monte Carlo expectation maximization algorithm for obtaining estimates of the parameters of interest. The goal of this model is to infer the connectivity matrix of a population of neurons. This method is highly promising, as it does not rely on linear assumptions of neuronal dynamics and has been tested extensively on simulated data. The main points of the model are summarized as follows (Volgelstein, et al., 2009); (Mishchencko, Vogelstein, & Paninski, 2011):

1. Spike: generalized linear model to capture the firing properties of individual neurons. Overall unknown parameters $\{\boldsymbol{w_i} = (w_{i1}, \dots, w_{iN}), k_i, b_i\}$ for hidden variable $n_i(t)$,

$i \leq N$.

- Denote the ith neuron's spiking activity at discrete time t as $n_i(t)$, $n_i(t) \sim Bernoulli[f(J_i(t)]$
- The spiking probability for the ith neuron is modeled by a nonlinear function $f(\cdot)$ of function $J_i(t)$. $J_i(t)$ is the summed input to neuron i at time t. The author used $f(J) = 1 - \exp(-e^J \Delta)$, where Δ is the inverse frame rate or the time interval size that scales the firing rate
- $J_i(t)$ is composed of various inputs, as mentioned above, including a baseline value b_i, external stimulus $S(t)$, spike influences $h_{ij}(t)$ detailing the influence of neuron j on neuron i; the influences are weighted by w_{ij}. Thus, $J_i(t) = b_i + k_i \cdot S(t) + \sum_{j=1, j\neq i}^{N} w_{ij} \cdot h_{ij}(t)$
- Model $h_{ij}(t)$ as an autoregressive process driven by the spike train of the jth neuron, $n_j(t)$. Thus $h_{ij}(t) = \left(1 - \frac{\Delta}{\tau_{ij}^h}\right) h_{ij}(t - \Delta) + n_j(t - \Delta) + \sigma_{ij}^h \sqrt{\Delta} \epsilon_{ij}^h(t)$, where τ_{ij}^h is the decay time constant, and it is treated as known and the same for all pairs (i, j), as is σ_{ij}^h

2. Calcium: conditional first-order hidden markov model for intracellular calcium concentration of individual neurons at time t with spike activity as modeled by $n_i(t)$. Overall unknown parameters $\{C_i^b, \tau_i^c, A_i, \sigma_i^c\}$ for hidden variable $C_i(t)$, $i \leq N$
   - $C_i(t) = C_i(t - \Delta) + (C_i^b - C_i(t - \Delta)) \frac{\Delta}{\tau_i^c} + A_i n_i(t) + \sigma_i^c \sqrt{\Delta} \epsilon_i^c(t)$
   - When there is no spiking, Calcium goes down to baseline level C_i^b
   - When $n_i(t)$ = 1, Calcium goes up by a fixed amount A_i, which is the impact

on calcium amplitude due to spike, then decays with time constant τ_i^c

3. Fluorescence: observed fluorescence $F_i(t)$ as a nonlinear function of Calcium with unknown parameters $\{\alpha_i, \beta_i, \gamma_i, \sigma_i^F\}, i \leq N$
   - $F_i(t) = \alpha_i S\big(C_i(t)\big) + \beta_i + \sqrt{(\sigma_i^F)^2 + \gamma_i S\big(C_i(t)\big)}\epsilon_i^F(t)$
   - $S(C) = C/(C + K_d)$ is a saturating function, modeled by a Hill function of the bound Calcium concentration (Orlandi, Stetter, Soriano, Geisel, & Battaglia, 2014)
4. MCEM for parameter estimation:
   - Unknown parameters $\theta_i = \{\boldsymbol{w_i}, k_i, b_i, \boldsymbol{C_i^b}, \tau_i^c, A_i, \sigma_i^c, \alpha_i, \beta_i, \gamma_i, \sigma_i^F\}$
   - Define $\tilde{\theta}_i = \{\boldsymbol{w_{ii}}, k_i, b_i, \boldsymbol{C_i^b}, \tau_i^c, A_i, \sigma_i^c, \alpha_i, \beta_i, \gamma_i, \sigma_i^F\}$ as our intrinsic parameters
   - Interested in finding the connectivity matrix $\boldsymbol{w} = \{\boldsymbol{w_i}, \dots, \boldsymbol{w_N}\}$
   - Use Monte Carlo Expectation-Maximization algorithm to estimate the parameters, which incorporates block-wise-Gibbs algorithm for sampling from joint neuron activity

2.1.1 Limitations

This method's accuracy increases with data availability, as it is model dependent. As our datasets contain time series that are all less than 600 seconds each, the method may not infer as accurately a connectivity matrix as we would hope. More importantly, the author uses 60Hz imaging rate, which we also do not have. The author mentions in his paper that

genetically encoded calcium indicators are under development in recent years, and would allow the signal-to-noise levels to approach near single spike accuracy. This particular method can be used to exploit data collected from such advanced imaging techniques. Therefore, it would be to any researchers' advantage to invest time in learning this method for future application. However, at the moment there are no implementation packages readily available. Given the complexity of this model and its parameter estimation algorithm, collaboration or consultation with the authors is highly recommended if one wishes to implement this method correctly. Finally, the method is in the process of being tested on real data, and its real world application performance has yet to be evaluated.

2.2 Cross-Correlation

Cross-correlation connectivity reconstructions are based on the assumption of linearity of neuronal dynamics; it uses Pearson's correlation. This method is among the standard methods in the problem field, and has been widely used by researchers (Garofalo, Nieus, Massobrio, & Martinoia, 2009). Cross-correlation is a function that assigns a score to each potential link between two time series, given by the largest cross-correlogram of lag τ between the series, $0 < \tau < t_{max}$ (Garofalo, Nieus, Massobrio, & Martinoia, 2009). In other words, it measures the similarity between one series and lagged copies of the other series as a function of the lag, and finds the maximum correlation. Garafalo et al. uses 150ms for t_{max}, with incremental value 0.1ms, while Stetter et al. uses 60ms, with similar incremental value. The goal of this method in this problem setting is to infer a directed connectivity matrix for a population of neurons, by finding the cross-correlation link value between all pairs of neurons.

We denote the cross-correlation function by XC. If X and Y are two discrete markov processes (i.e. two fluorescence time series), and S represents the set of values in X and Y, then

$$XC_{Y\to X} = \max_{\tau=0,\ldots,t_{max}} \{corr(x_S, y_{S-\tau})\}$$

returns the cross-correlation of Y's influence on X.

2.2.1 Limitations

Real life phenomena are rarely linearly related. Thus, linear causality measures applied to such a complex system of information that is a neuron network can hardly be reliable. Though many implementation packages are readily available in statistical analysis software, the use of this method should always be compared to other methods or restricted to exploratory analysis, as there is no ground truth of network topology available to us. As shown by Stetter et al., in their comparison of XC to other connectivity methods, XC inferred a connectivity that is too clustered, which did not reflect the true nature of their simulated data. However, XC are of great use in other applications including finding the relative strength of synchrony of close neighboring neurons (Stetter, Battaglia, Soriano, & Geisel, 2012).

2.3 Transfer Entropy

Transfer Entropy is an information theoretic measure (Vicente, Wibral, & Lindner, 2011). It is used to extract causal relationships from two time series. With respect to the

cross-correlation method, transfer entropy is sensitive to both linear and non-linear interactions, as it is model free, meaning it makes no assumptions to the underlying neuronal interaction. The method incorporates directional and dynamical information by using the history of both time series in its calculations. Mathematically, if we assume that two time series, X and Y, can be represented by Markov processes, then TE is a measure of deviation from the generalized Markov condition

$$p(x_{t+1}|x_t^n y_t^m) = p(x_{t+1}|x_t^n)$$

where $x_t^n = (x_t, \dots, x_{t-n+1})$, $y_t^m = (y_t, \dots, y_{t-m+1})$, n, m are orders of the Markov processes and p denotes the transition probabilities conditioned to the past n, m observations of the Markov processes X and Y, respectively. This equation is fully satisfied when the dynamic of X is independent of the m past time points of Y. When it is not satisfied, the departure can be measured (Schreiber, 2000) as

$$TE_{Y\to X} = \sum_{x_{t+1}, x_t^n, y_t^m} p(x_{t+1}, x_t^n, y_t^m)\log\left(\frac{p(x_{t+1}|x_t^n, y_t^m)}{p(x_{t+1}|x_t^n)}\right)$$

which we may interpret as system Y adding predictability to system X. In other words, the connectivity we measure is "improved predictability" of X because of Y (Stetter, Battaglia, Soriano, & Geisel, 2012). Low TE value implies that y_t^m has little to no influence on the transition probabilities of X, while high TE values indicate the time series Y influences times series X. Similarly, TE is zero if two time series have the same transition probabilities. Due to its inherent asymmetry, $TE_{Y\to X}$ is not the same as $TE_{X\to Y}$.

Using a little algebra and substitution, the equation becomes (Tenkanen, 2008)

$$TE_{Y\to X} = \sum_{x_{t+1}, x_t^n, y_t^m} p(x_{t+1}, x_t^n, y_t^m)\log\left(\frac{p(x_{t+1}, x_t^n, y_t^m)p(x_t^n)}{p(x_t^n, y_t^m)p(x_{t+1}, x_t^n)}\right)$$

which can be calculated easily if X and Y are discrete. The measure is highly interpretable, and is adequate for determining the direction of information flow among two time series (Kaiser & Schreiber, 2002).

Transfer entropy has been used to find effective connectivity of different brain regions (Vicente, Wibral, & Lindner, 2011), functional connectivity in cortical networks using micro-electrode array data (Garofalo, Nieus, Massobrio, & Martinoia, 2009), information transfer between auditory cortical neurons (Gourevitch & Eggermont, 2007), and calcium signaling patterns under different cellular conditions (Pahle, Green, Dixon, & Kummer, 2008), to name a few.

Most recently, Orlandi et al., and Stetter et al. have furthered the work of Garofalo et al. to apply transfer entropy to calcium imaging data. Given the challenges present in this type of data, these researchers have derived a generalized transfer entropy as an extension of TE to overcome the challenges.

2.3.1 Generalized Transfer Entropy

The goal of generalized transfer entropy is the same as the Bayesian and cross-correlation methods; it is to yield a connectivity matrix of TE values that represents a directed functional connectivity network of neurons whose activities were observed under calcium imaging techniques. Standard transfer entropy is modified in two major areas and several smaller areas to accommodate calcium imaging data (Stetter, Battaglia, Soriano, & Geisel, 2012).

1. Same time bin: Since calcium imaging acquisition rate is much slower than synaptic activity, the fluorescence measured at each time point can be thought of as a time bin.

The authors proposed to evaluate p, which denotes the transition probabilities, conditioned to the past k observations of the markov process X, current observation Y, and $k-1$ past observations of Y, to account for same time bin causal interactions between neurons.

2. Conditioning level: The authors observed that the neuronal network switches between dynamical states as a whole. They call them bursting and non-bursting states of the network. During burst, the network is excitable and the directed functional connectivity can be hard to detect. During a non-burst phase, the activities of neurons and their interactions can be better observed. Hence, TE evaluation is restricted to time ranges in which the network is consistently in the non-bursting dynamical state. For a graphical explanation, please refer to Mishchenko et al.'s paper, Figure 11 (Mishchencko, Vogelstein, & Paninski, 2011). The separation of states can be achieved by calculating the average signal of the entire network of N neurons:

$$g_t = \frac{1}{N}\sum_{i=1}^{N} x_i(t)$$

Then, a threshold $\tilde{g}$ is chosen based on the fluorescence amplitude histogram of the network (e.g. Figure 3). This is achieved by taking the conditioning level to be approximately two standard deviations above the mean of the normal-looking part of the graph. All data points at time t for which $g_t < \tilde{g}$ are included in the analysis.

3. Quantize continuous fluorescence: the probabilities in transfer entropies are evaluated at discrete values. Since fluorescence (after processing) is continuous data, we need to quantize the time series into B discrete levels. The authors fixed $B = 3$, but in this

paper we will use $B = 4$. The rationale is we would like to have the resulting amplitude width of each discrete level to be close to twice the standard deviation of the fluorescence signal.

4. Final generalized transfer entropy:

(Orlandi, Stetter, Soriano, Geisel, & Battaglia, 2014)

$$GTE_{J\to I}(g_t < \tilde{g})$$

$$= \sum_{i_{t+1}, i_t^{(k)}, j_{t+S}^{(k)}} p\left(i_{t+1}, i_t^{(k)}, j_{t+S}^{(k)} \middle|\, g_{t+1} < \tilde{g}\right) \log\left(\frac{p(i_{t+1} \middle| i_t^{(k)}, j_{t+S}^{(k)}, g_{t+1} < \tilde{g})}{p(i_{t+1} \middle| i_t^{(k)}, g_{t+1} < \tilde{g})}\right)$$

Where I and J represent quantized fluorescence time series, $i_t^{(k)}$ is a vector in time that has length k, representing the underlying fluorescence process $x_t^n = (x_t, \dots, x_{t-n+1})$, and S is the shift variable that can take values 0 or 1. If $S = 1$ then we include same time bin interaction in our analysis. If $S = 0$ then this aspect of the model resemble the standard transfer entropy. According to the authors, $k = 2$ is enough to allow generalized transfer entropy to separate actual interactions from other signal disturbances.

2.3.2 Limitations

Although the generalized transfer entropy addresses several limitations to the TE method, there still poses other challenges. First, generalized transfer entropy is a new method lacking in standardized implementation software (there exists C++ and MATLAB tools only), however, the algorithm is not difficult to code from scratch. The choice of k can be of some difficulty to researchers. Though time lag is somewhat incorporated into transfer entropy by

way of looking at both the time series' history, choosing k too small may result in non-accurate causal influence estimates (Vicente, Wibral, & Lindner, 2011). Moreover, though the method is model free, the data set should still be reasonably large. As well, the conditioning level decreases the dataset, which should be taken into consideration. This method is able to deal with sequences with both excitatory and inhibitory data, however, it is unable to identify the connection type by itself. Finally, as with all previous methods for connectivity reconstruction, there is no ground truth with which we can compare our reconstructed results to. Nevertheless, given its interpretability, model-free nature, and fairly straight-forward implementation, this method is chosen for analysis on real data in this paper.

3. Research Design

Three sets of data were kindly provided by Dr. Michael J Higley, Yale School of Medicine. The data were collected using calcium imaging and fluorescence indicators on mice under anesthetics. The data underwent pre-processing before analysis. We then used the extension of transfer entropy to reconstruct the directed functional connectivity of our network. The presence of a directed edge from neuron i to j imply a direct causal influence by the source node i to the sink node j. The method can be applied to data with both excitatory and inhibitory synapses, however, identification of type of connection (i.e. inhibitory or excitatory) is difficult as there is no prior information on neuronal type nor procedure that collected excitatory activities only of the same set of neurons (Orlandi, Stetter, Soriano, Geisel, & Battaglia, 2014)

To interpret the results, the reconstructed functional connectivity matrix was ranked, and a thresh-hold was used to maintain the top 5% of connections, producing an adjacency matrix (as recommended by Setter et al., 2012). The adjacency matrix A has entries $a_{ji} \in \{0,1\}$, where 1 means a connection from neuron j to i which is in the top 5% of all connections, and 0 means no connection or a weak connection relative to other connections. We then can use this adjacency matrix to illustrate our findings using a directed graph.

To assess our findings, the average full cluster coefficient over all neurons was calculated as a summary statistic for our directed network (Fagiolo, 2007):

$$CC = \langle \frac{(A + A^T)^3_{ii}}{2T_i} \rangle_i$$

$$where \;\; T_i = d_i^{total}\left(d_i^{total} - 1\right) - 2d_i^{bidirect}$$

$$(A + A^T)^3_{ii} = \sum_j \sum_h (a_{ij} + a_{ji})(a_{ih} + a_{hi})(a_{jh} + a_{hj})$$

An in-degree of neuron i is the number of edges going into i, which can be calculated by taking row sum of column i of the adjacency matrix. An out-degree of neuron i is defined as the number of edges going out of i, which can be calculated by taking the column sum of row i of A. Then, d_i^{total} is the total-degree of node i; the sum of in-degree and out-degree of node i. Whereas $d_i^{bidirect}$ is the number of bi-directional edges node i has. When i has an edge going into j and j has edge going into i, then this is a bi-directional edge for i. The cluster coefficient measures the phenomena that is intrinsic to networks: forming circles of connected nodes (Fagiolo, 2007). The full cluster coefficient is an extension of cluster coefficient from undirected graphs to directed graphs.

Then, hubs of causal connectivity (Stetter, Battaglia, Soriano, & Geisel, 2012) were identified by finding the neurons with highest in-degrees. Finally, randomization was used to identify statistically significant non-random features of the network.

Furthermore, to set a direction for future analysis and methodology development, we compared results of our evaluations based on different Markov orders (k) for the Markov processes (the fluorescence sequences) of the first data set. Additionally, we compared the adjacency matrix of generalized transfer entropy evaluated on pre-processed raw data versus non-processed raw data for the second data set. We hypothesize, given larger data observations and higher frame rate in data set two, that using raw-data does not perform worse than using pre-processed data. Finally, we compared results of reconstruction based on varying conditioning levels to check robustness of our reconstruction. This final comparison

is not shown in this paper as we verified that the inferred connectivity features were consistent if conditioning level remained close to the original choice and not further than two standard deviations away (Stetter, Battaglia, Soriano, & Geisel, 2012).

3.1 Data Processing I

The first dataset we will explore and analyze contains spontaneous activity of 98 neurons over 3500 image frames, captured at 14.8Hz. Both raw data and pre-processed neuropil corrected $\Delta F/F$ data are given. A number of past studies have shown that neuropil-corrected $\Delta F/F$ can be interpreted as time series reflecting spike activity (Goltstein, Montijn, & Pennartz, 2015). However, preprocessing is not always necessary in order to use generalized transfer entropy. Nevertheless, Setter et al. claims that even a basic discrete differentiation to fluorescence time series can isolate potential spike events, as well as improve signal-to-noise ratio, which allows for a better sampling (based on conditioning level) of distributions with limited number of data points (Stetter, Battaglia, Soriano, & Geisel, 2012). Since our imaging video is only four minutes long and has a low frame rate, the neuropil-corrected $\Delta F/F$ was used (98 neurons over 3456 frames, as 44 frames were used for baseline calculations).

3.2 Data Processing II

The second dataset contains spontaneous activity of 69 neurons over 15000 image frames, captured at 28.38Hz. Only raw data was given and we need to pre-process it. Many researchers (Golstein et al., 2015; Montjin et al., 2014; Jia et al., 2010) have calculated their

$\Delta F/F$ (more precisely, $(F_i - F_{baseline\ of\ i})/F_{baseline\ of\ i}$) differently, with baseline window preceding image frame i ranging from 3s to 30s, and mean value taken over lowest value to 50% of values in this window. Many baseline values were tried in this dataset, ranging from 10% of 3s window to 50% of 3s window. Ultimately a 30% of 3s window was chosen to be the criteria for baseline calculation. In this dataset, we will also compare reconstruction based on raw data versus reconstruction based on processed data to show why this pre-processing step is important in reconstruction; however, with higher frame rate and better signal-to-noise ratio, this step may become unnecessary.

3.3 Data Processing III

While it is known that techniques to infer functional connectivity networks seem to rely on investigation of spontaneous activity (Garofalo, Nieus, Massobrio, & Martinoia, 2009), the stimulus data set can still be of use. This third dataset contains the same neurons as dataset two, but activity was only captured over 13785 image frames. The stimulus orientation remained at 30 degrees throughout the experiment, but contrast of stimulus changed 11 ways. The stimulus was initially off for approximately 4s, then on for 2s, then off for 4s, for each contrast level. The experiment was repeated seven trials. We propose a plan of first obtaining the $\Delta F/F$ (30% of 3s window as baseline) for each neuron's time series, then dissecting each time series into 77 segments, each containing one trial over one stimulus. We then take trial average per contrast level as the $adjusted\ \Delta F/F$ for each neuron. We do so for all contrast levels. Note that each segment contains 2 seconds of stimulus on and 4 seconds of stimulus off.

4. Analysis and Results

4.1 Results I

We first applied generalized transfer entropy to the reconstruction of a network based on 98 neurons over almost four minutes of spontaneous activity (Figure 1). The average fluorescence signal g_t is calculated (Figure 2) and its frequency distribution plotted (Figure 3). The distribution is right-skewed, as expected, displaying towards the left side times during which the network was in non-bursting phase, and towards the right side times during which the network was in synchronous burst. Based on this plot we chose a conditioning level $\tilde{g}$=0.1974 which would exclude the right-tail of high average fluorescence amplitudes. Then, reconstruction analysis using generalized transfer entropy was applied on the data set of 98 time series. We initiated the algorithm using B=4 (quantize fluorescence amplitudes into 4 categories), S=1 (consider same time-bin interaction), and k=2 (markov order considering past two time point events). A reconstructive matrix was generated indicating the TE causal influence value between each pair of neurons. Recall that TE for $j \to i$ is often not the same as TE for $i \to j$. Moreover, the diagonal terms for the reconstructive matrix are not for interpretation, because we are not considering causal influence between a neuron and itself. We threshold the connectivity matrix to retain the top 5% of connections, and produce an adjacency matrix illustrated by a directed graph (Figure 4). The average in-degree for the network is 5 and average full cluster coefficient is 0.182. The distribution of full-cluster coefficients and in-degrees for the set of 98 neurons is displayed in Figure 7a.

4.1.1 Comparison to randomized networks

We do not know what the functional organization or structure of the network of neurons actually looks like. Therefore, we use randomization to assess our findings. At least, we may determine if our reconstructed connectivity is a deviation from random connectivity. There are two types of randomization we can do to make such comparisons. First, we may compare our reconstruction with a fully randomized network by preserving the number of connections in the adjacency matrix, then mixing up the source and sink nodes (Figure 6 left). First row of Figure 7a shows the distribution of cluster coefficients and in-degree of reconstructed network, and second row shows the same properties of the fully randomized network. We observe that while the fully randomized network has cluster coefficient distribution somewhat normal and in-degree following the Poisson distribution (Newman, Trogatz, & Watts, 2001), our reconstructed network deviates heavily from such distributions. This indicates our findings of network features are not random. In particular, TE detects large cluster coefficients for certain nodes but small or no clustering for other nodes. The overall clustering coefficient for the network is 0.182, significantly larger than for fully random network (0.024).

A second method of randomization preserves the total connections and the out-degree of each node, and partially randomizes the network based on randomization of in-degrees. Bottom row of Figure 7a we can see that the partially randomized network has similar distributions of cluster-coefficient and in-degrees as fully randomized networks. Therefore, our reconstructed network features are not random. In particular, using in-degrees, we found sink nodes with larger than average in-degrees and highlighted them in red (Figure 8). While

the average for both partially randomized network and our reconstructed network was 5, the reconstructed network displayed sinks with more than 20 in-degrees, a phenomena non-existent in the randomized graph.

4.1.2 Comparison of network reconstructions based on different Markov orders

In Figure 5 we plotted the reconstructed network based on $k = 3$ and $k = 4$. The result is sparser connectivity as indicated by visual observation. We see that many nodes are left "untouched" by the links, which is consistent with the understanding that neuronal coding in V1 exhibits sparse coding (Montijn, Vinck, & Pennartz, 2014). Their in-degree and full cluster coefficient distributions are shown in Figure 7b. We see that the distributions are far from random. Moreover, the increase in number of nodes with no in-degrees can also substantiate our claim above that there seems to be more sparseness. For this paper we will continue to use $k = 2$. The authors who derived this method indicated in their analysis using simulated data which has ground-truth available that a Markov order of 2 is able to achieve a performance level ranging between 40% to 80% and only 10% false positive links, for any clustering type and conditioning level. However, in the future, it would be worthy to explore the statistical properties and effects of increasing markov order in neuronal connective reconstruction.

4.2 Results II

For the second set of spontaneous data, we do the same thing as we did for the first set of data (Figure 9). The results provide validation for our findings previously in data set one. Our reconstructed connectivity graph (Figure 10 top) shows non-random features that are not displayed in both randomized networks. This phenomena is clearly seen by the distribution of full cluster coefficients and in-degrees of 69 neurons for reconstructed network compared to both randomized networks (Figure 11 top). While all three graphs have an average in-degree of 3.5, our reconstructed network has in-degree values over 10, and these nodes are highlighted in blue (Figure 11 bottom).

4.2.1 Comparison of network reconstructions using pre-processed and raw data

In Figure 12 we show the results of reconstruction using raw data that was not pre-processed using a baseline fluorescence value. The average full cluster coefficient is 0.116, higher than what we found with pre-processed data and a slightly different set of neurons with in-degrees over 10 was found. Moreover, the distribution of in-degrees (Figure 12 bottom) is similar to that of pre-processed data. Such observations do not tell us if pre-processing is necessary, but the findings do not reject our hypothesis that using raw-data does not perform any worse than pre-processed data, given higher frame rates and larger data size. However, it is known that pre-processed data is able to increase signal-to-noise ratio, and such a feature is not without its advantages.

4.3 Results III

We briefly analyze the dataset with stimulus indicators. We see that for each contrast level, different sink nodes with greater than 10 in-degrees are identified (Figure 13). However, the dataset for each contrast level is very small (trials average totaling 6 seconds), and this may cause biased estimation of TE values. Nevertheless, it is notable to say that different contrast levels seem to display different patterns of connectivity, with a few neurons consistently appearing to have more than average in-degrees. For example, neuron 44, neuron 4 and neuron 60. The cluster coefficient for all network reconstructions over 11 contrast levels is consistently in the 0.20 to 0.35 range. While not displayed, the randomized networks consistently had lower cluster-coefficients in the range of less than 0.10, with in-degrees for each node less than 10. These results indicate non-random patterns of connectivity for different stimulus.

5. Discussion

We have used a model-free, computationally feasible method to find the directed functional connectivity of our two populations of neurons, without inferring spike trains from the data. The connectivity patterns we obtained are non-random. Certain neurons in each data set displayed higher number of in-degrees than others, and the phenomena is different from random patterns. While some neurons displayed high full cluster correlations by having a community of connected nodes, which is also non-random. These significant findings suggest that this method is able to capture some interaction, specifically, causal influence, among the neurons in the populations.

The neurons with above-average in-degree of connectivity are seen as hubs of causal connectivity. We can use its first neighbors to define a community. It has been found that synchronization within these communities based around hubs are stronger than communities based around nodes with less in-degree. As well, a direct stimulation of hubs can trigger the synchronous reactions of its community. Researchers also found that synchronous activities are associated to functional connectivity with higher overall average cluster coefficient. However, it is also associated with less overlap with the underlying structural connectivity of the neuron population (Stetter, Battaglia, Soriano, & Geisel, 2012). Nevertheless, the chance of hubs who are functionally connected also being structurally connected is significantly larger than random networks. As a result, future work in this field should involve the analysis of both structural connectivity and

patterns of functional connectivity. The incorporation of stimulus (cognitive activation, as opposed to spontaneous activity) should also be explored more in depth.

In the past, brain properties have been studied through brain region interactions and individual neuron behaviors. Ensembles of neurons have not been vastly explored (McIntosh, 2010). Scientists believe that a key to further understand how the brain controls thought, perception and memory is through learning how neurons work together. This paper aims to use one of few developed methods for calcium imaging data to find any connectivity among an ensemble of neurons. This project adds to current research on neuron connectivity and functional organization by using real data to test the methodology. Now that we have found non-random topology of neuron population, what can we do with it?

This method's main output is an adjacency matrix which we can plot and observe visually. Therefore, this method may be fit for exploratory analysis. Reconstructed neuronal connectivity provides information on how the neurons work together given a certain period of time and frame rate. We may use it to compare with its structural connectivity. Furthermore, we may use experimental methods, in conjunction with reconstruction of functional connectivity, to distinguish between inhibitory and excitatory neurons. It is known that anything that affects a specific brain region will ultimately affect the entire brain network. Perhaps it is analogous with neuron networks. We can hypothesize that diseases, disorders, and deficits can reflect an abnormal or damaged network of neurons in a specific region of the brain. We can learn about the dysfunctional neuron network by comparing its connectivity to network operations by

normal, healthy neuron networks. Some researchers have found that spontaneous, resting, brain activity are useful for finding the brain's functional blueprint (McIntosh, 2010). We may also hypothesize that resting neuron population activity are the blueprint for neuronal network interaction. Researchers have found that reduced functional connectivity correlates with a decline in executive function and processing speed. For example, Alzheimer's disease is associated with reduced functional connectivity (McIntosh, 2010). Perhaps it is useful to apply the same concept to neuronal populations, and see if such discrepancies exist between normal and dysfunctional brains. By locating the population of neurons with lower functional connectivity, we may be able to pinpoint the source of disease, disorder, or deficit.

6. Conclusion

In this paper we have established that generalized transfer entropy is a method of reconstruction for neuronal connectivity that works. We have found non-random features of our network of neurons and can use such findings to further our research. Generalized transfer entropy is one of many methods that can reconstruct interactions, or connectivity, between neurons with calcium imaging data. However, given our lower frame rate and potential poor signal-to-noise ratio, a model-free method that makes no assumption of linearity or interaction gives flexibility and robustness.

Furthermore, the model does not require deconvolution. Other approaches have emphasized on the need to reconstruct spike trains, but techniques to do so are complicated and sometimes impossible to optimize, due to lack of prior testing (Moreaux & Laurent, 2008). This pre-processing step is not needed with generalized transfer entropy. The method performs efficiently and thus the need to pull out spike trains is unnecessary, even if signal-to-noise is good enough.

There are some limitations to this field of study and to this method specifically. First of all we were only able to compare two neurons at a time. This method does not consider higher dimensions of analysis. Secondly, though this method has been established, there is no standard implementation. In other words, we have to conduct many sensitivity analysis on the data, and on parameter initialization. This is partly due to the way experiments are conducted and the difference in data collected. Also, it is due to lack of software or analysis packages. Furthermore, the true topology of the network

is unknown and therefore validation of method is non-existent, except through comparison to other methods or to the null (via randomization). Finally, the method cannot differentiate between types of neurons. However, with the help of a considerate experimental design, this is possible.

In many research papers, the connectivity reconstructed using transfer entropy is known as functional connectivity, not effective connectivity (Friston, 2011). However, in many other research papers, for example (Vicente, Wibral, & Lindner, 2011), the method is known to reconstruct effective connectivity. Effective and functional connectivity are different network connectivity, and the use of the two terms interchangeably or non-agreeably creates confusion in this field of study.

References

Averbeck, B. B., Latham, P. E., & Pouget, A. (2006, May). Neural correlations, population coding and computation. *Nature*.

Blaettler, F., Kollmorgen, S., Joshua, H., & Hahnloser, R. (2011). Hidden markov models in the neurosciences. *InTech*.

Blumenthal, J., Megherbi, D. B., & Lussier, R. (2014). Unsupervised machine learning via hidden markov models for accurate clustering of plant stress levels based on imaged chlorophyll fluorescence profiles and their rate of change in time. *IEEE*.

Chamroukhi, F., Same, A., Aknin, P., & Govaert, G. (2011). Model-based clustering with hidden markov model regression for time series with regime changes. In IEEE (Ed.), *International Joint Conference on Neural Networks.* San Jose.

Cohen, M. R., & Kohn, A. (2013). Measuring and interpreting neuronal correlations. *Nature Neuroscience*.

Fagiolo, G. (2007). Clustering in complex directed networks. *Physics Review*.

Friston, K. J. (2011). Functional and effective connectivity: a review. *Brain Connectivity, 1*.

Froudarakis, E., Berens, P., Ecker, A. S., Cotton, J. R., Sinz, F. H., Yatsenko, D., . . . Tolias, A. S. (2014, June). Population code in mouse V1 facilitates readout of natural scences through increased sparseness. *Nature Neuroscience, 6*.

Garofalo, M., Nieus, T., Massobrio, P., & Martinoia, S. (2009, August 4). Evaluation of the performance of information theory-based methods and cross-correlation to estimate the functional connectivity in cortical networks. *PLos ONE, 8*.

Goltstein, P. M., Montijn, J. S., & Pennartz, C. M. (2015, February 23). Effects of isoflurane anesthesia on ensemble patterns of Ca activity in mouse V1: reduced direction selectivity independent of increased correlations in cellular activity. *PLoS ONE*.

Gourevitch, B., & Eggermont, J. J. (2007). Spatial representation of neural responses to natural and altered consepecific vocalizations in cat auditory cortex. *Journal of Neurophysiology*.

Jia, H., Rochefort, N. L., Chen, X., & Konnerth, A. (2011). In vivo two-photon imaging of sensory-evoked dendritic calcium signals in cortical neurons. *Nature Protocols*.

Kaiser, A., & Schreiber, T. (2002). Information transfer in continuous processes. *Physica D: Nonlinear Phenomena, 166*, 43-62.

Korjus, K. (2011). *Causality measures in neuroscience: wiener-granger causality and transfer entropy applied to intracranial EEG data.* Manchester.

Kwan, A. C. (2010). Toward reconstructing spike trains from large-scale calcium imaging data. *HFSP Journal*.

McIntosh, A. R. (2010). Moving between functional and effective connectivity.

Mishchencko, Y., Vogelstein, J. T., & Paninski, L. (2011). A bayesian approach for inferring neuronal connectivity from calcium fluorescent imaging data. *The Annals of Applied Statistics*.

Montijn, J. S., Vinck, M., & Pennartz, C. M. (2014, June 02). Population coding in mouse visual cortex: response reliability and dissociability of stimulus tuning and noise correlation. *Frontiers in Computational Neuroscience, 8*.

Moreaux, L., & Laurent, G. (2008). A simple method to reconstruct firing rate from dendritic calcium signals. *Frontiers in Neuroscience*.

Newman, M., Trogatz, S., & Watts, D. (2001). Random graphs with arbitrary degree distributions and their applications. *Physical Review E, 64*, 1-17.

Orlandi, J. G., Stetter, O., Soriano, J., Geisel, T., & Battaglia, D. (2014, June). Transfer entropy reconstruction and labeling of neuronal connections from simulated calcium imaging. *PLoS ONE, 9*.

Pahle, J., Green, A. K., Dixon, C. J., & Kummer, U. (2008). Information transfer in signaling pathways: a study using coupled simulated and experimental data. *BMC Bioinformatics*.

Rabiner, L. R. (1989, February). A tutorial on hidden markov models and selected applications in speech recognition. *Proceedings of the IEEE, 77*.

Rama, J. A. (2013). *Clustering neuronal activity from fluorescent simulated traces and fluorescence calcium images by inferring spicular neuron activity.* Barcelona.

Schreiber, T. (2000). Measuring information transfer. *Physical Review Letters, 85*, 461-464.

Stetter, O., Battaglia, D., Soriano, J., & Geisel, T. (2012, June). Model-free reconstruction of excitatory neuronal connectivity from calcium imaging signals. *PLoS Computational Biology, 8*.

Stevenson, I. H., & Kording, K. P. (2011, February). How advances in neural recording affect data analysis. *Nature Neuroscience, 14*.

Tenkane, A. (2008). *Transfer entropy: a presentation in the information theory seminar.* Department of Information Technology, University of Turku.

Vicente, R., Wibral, M., & Lindner, M. (2011). Transfer entropy - a model-free measure of effective connectivity for the neurosciences. *Journal of Computational Neuroscience, 67*, pp. 30-45.

Volgelstein, J. T., Watson, B. O., Packer, A. M., Yuste, R., Jedynak, B., & Paninski, L. (2009, July). Spike inference from calcium imaging using sequential monte carlo methods. *Biophysical Journal, 97*, pp. 636-655.

Zylberberg, J., & Shea-Brown, E. (2014). When does recurrent connectivity improve neural population coding. *BMC Neuroscience*.